

Performance Analysis of Scroll Compressors Using CO₂ Refrigerant

Authors: *Mihoko Shimoji** and *Toshiyuki Nakamura***

1. Introduction

We manufactured a prototype of a large-capacity scroll compressor that uses CO₂ refrigerant, evaluated the performance of it, and analysed losses using a simplified model based on a basic test. As a result, the compressor input power levels in both the measurement and analysis agreed, although with a difference of approx. 3%, in the range of rotational speed from 30 to 100 rps. The availability of the analysis method was thus verified.

2. Specifications of the Prototype

For examination of the performance of a CO₂ compressor when used for air-conditioning (cooling), the authors manufactured a prototype compressor that uses CO₂ refrigerant, which is equivalent to 10HP and based on a mass-produced scroll compressor that uses R410A refrigerant.

The stroke volume of this compressor was designed to be approximately one-third ($24 \times 10^{-6} \text{ m}^3/\text{rev}$) that of a R410A compressor, since the cooling capacity of CO₂ refrigerant per unit stroke volume is about three times that of the R410A refrigerant.

The operating pressure of CO₂ refrigerant is three times higher than that of R410A refrigerant and fluctuates with a large peak-to-bottom difference, resulting in a high operating load. For this reason, the reliability of the compressor was ensured by increasing the strength of the components such as compression part, and also by reinforcing the bearing support structure. In addition, for the prevention of refrigerant leakage, tip seals were applied to the axial leakage gaps in the scroll-wrap tips. Sliders⁽¹⁾ were used for sealing the leakage gaps in the radial direction on the scroll wrapside. (The turning radius of the orbiting scroll was changed during operation and this presses the orbiting scroll against the fixed scroll.)

3. Performance Evaluation of the Prototype

3.1 Evaluation conditions

Table 1 shows the evaluation conditions and stroke volume of the prototype. We evaluated the performance on the assumption that the prototype will be used for air-conditioning (cooling).

Table 1 Test conditions and stroke volume of the prototype

| Item | Value |
|---------------------|--|
| Suction pressure | 4 MPa |
| Discharge pressure | 10 MPa |
| Compression ratio | 2.5 |
| Suction temperature | 15°C |
| Rotational speed | 30rps/60rps/100rps |
| Stroke volume | $24 \times 10^{-6} \text{ m}^3/\text{rev}$ |

3.2 Results of the performance evaluation

Figure 2 shows the volumetric efficiency and overall adiabatic efficiency of the prototype under the operating conditions shown in Table 1. The efficiencies shown in Fig. 1 are the results of dividing the efficiency levels at each rotational speed by the efficiency level at 60 rps. The efficiency dropped significantly at low rotational speeds: the volumetric efficiency and overall adiabatic efficiency at 30 rps became lower than those at 60 rps by 17% and 16%, respectively.

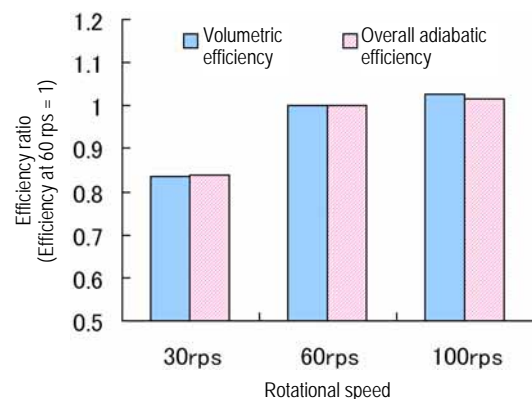


Fig. 1 Efficiency of the prototype

In the following chapters, we discuss loss analysis, using the methods described below to clearly identify the relationship between rotational speed and efficiency.

4. Loss Analysis

The input power to the scroll compressor is divided into theoretical compression power and various types of losses, as shown in Fig. 2. The respective types of losses are calculated based on pressure changes in the compression chamber. We are concerned here only with analysis methods of major losses.

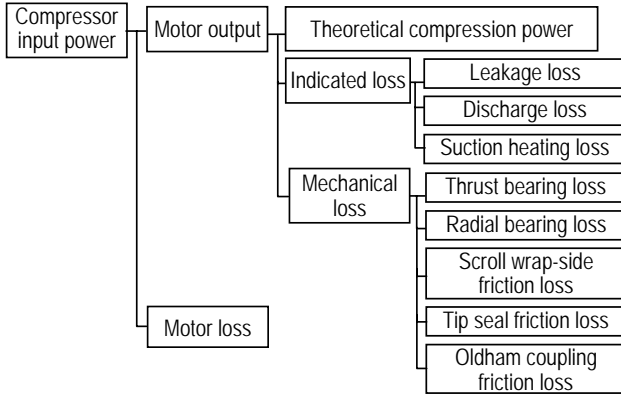


Fig. 2 Diagram of compressor input power

4.1 Basic equations for the compression stroke

On the basis of the laws of conservation of mass and of conservation of energy and the changes in volume in the compression chamber, the changes in quantity of state in the compression chamber are expressed by equations (1) and (2) below.

$$dM = dM_{in} - dM_{out} \quad (1)$$

$$dU = \frac{1}{M} \{ (h_m - h) dM_m + P v \cdot dM - P \cdot dV \} \quad (2)$$

where, U = internal energy, M = mass, h = specific enthalpy, P = pressure in compression chamber, v = specific volume, V = volume of the compression chamber, suffix "in" indicates influx of refrigerant gas, and suffix "out" indicates outflow of refrigerant gas.

The basic equations in (1) and (2) above and changes in volume were used as simultaneous equations and the quantity of state in the compression chamber was determined by integration, for each compression chamber. Refprop7 is used as the refrigerant physical property program.⁽²⁾

4.2 Leakage analysis model

The leakage flow rate ΔG of CO_2 refrigerant flowing through micro gaps is determined by multiplying the mass flow rate G_{ad} per unit area obtained by the equation of isentropic flow of the convergent nozzle by the leakage area S and leakage flow coefficient α , which is described below.

$$\Delta G = \alpha S_c G_{ad} \quad (3)$$

The leakage gap in the axial direction of the scroll wrap tip and the leakage gap in the radial direction of the scroll wrap side were assumed to have been sealed with tip seals and the slider respectively. The refrigerant gas were assumed to leak only through the gap created at the side of the tip seal section. The dimensions of the gaps in the respective compression chambers were assumed to be the same taking account of thermal expansion and frame deformation under pressure during

operation.

The flow coefficient α was determined in such a way that the left-hand side (leakage flow into the suction side calculated from measurement data) of the equation (4) was equal to the right-hand side (leakage flow into the suction side determined by calculation). The flow coefficient α thus obtained was applied to all the leakage gaps.

$$\rho_{sh} V_{st} N - G_{exp} = \alpha \overline{S_c G_{ad}} \quad (4)$$

The first term on the left-hand side of equation (4) above is the amount of refrigerant circulating, determined by multiplying the density at a gas temperature measured immediately before suction into the compression chamber ρ_{sh} , by the stroke volume V_{st} and the rotational speed N . The second term on the left-hand side is the measured amount of refrigerant in circulation G_{exp} . The right-hand side indicates the leakage flow into the suction side, calculated periodically by equation (3) and averaged for a single rotation.

4.3 Discharge model

When the pressure in the compression chamber becomes higher than the discharge pressure, as shown in Fig. 3, the discharge valve opens to release refrigerant gas.

Using the Bernoulli equation (5) below, the pressure rise ΔP during discharge was determined on the assumption that the discharge is a permanent flow of incompressible fluid without friction.

$$\Delta P = \xi \frac{1}{2} \rho u_d^2 \quad (5)$$

In equation (5) above, ρ is the gas density in the compression chamber, ξ is the discharge loss coefficient, and u_d indicates the flow velocity at the opening area S_d at the discharge valve, shown in Fig. 3. It was also assumed that the valve lift would be at maximum during the gas outflow. The discharge loss coefficient ξ was set at 4.8 by taking into consideration the contraction of gas at the discharge port and also the inlet loss, bend loss and outlet loss.

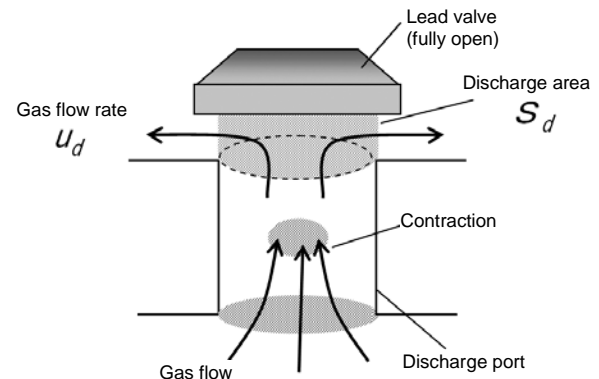


Fig. 3 Discharge model

4.4 Thrust bearing loss model

The friction loss W_{TH} of the orbiting scroll and the thrust bearing is expressed by equation (6) below. In equation (6), F is the average gas load in the thrust direction, calculated from the pressure in the compression chamber, μ is the friction factor, r is the orbital radius and N is the rotational speed. The value for the friction factor μ above was determined by experiment, using the method of measuring the friction coefficient shown in Fig. 4, with lubricant dropped in a CO₂ refrigerant environment.

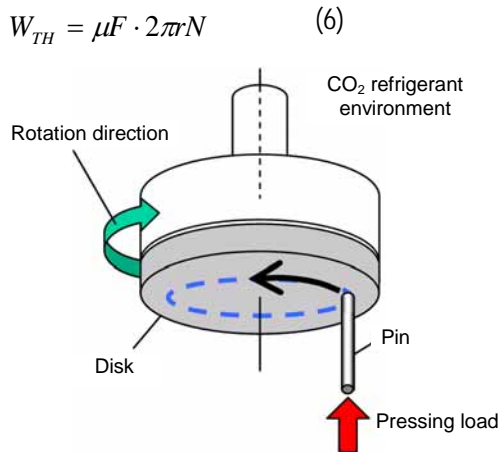


Fig. 4 Pin-on-disk type friction factor measuring equipment

5. Results of Loss Analysis

Table 2 shows the prediction errors in the compressor input power values from analysis results under the evaluation conditions shown in Table 1. In Table 2, the prediction error in compressor input power is expressed by the equation $\gamma = (\text{Analysis input} - \text{Measurement input}) / (\text{Measurement input}) \times 100[\%]$.

Table 2 Prediction error of input power

| Rotational speed | 30 rps | 60 rps | 100 rps |
|---|--------|--------|---------|
| Prediction error of input power: γ | +3.4 | -3.0 | -0.5 |

Table 2 indicates that the compressor input power levels in both the measurement and analysis agreed, albeit with a difference of approximately 3%, in the range of rotational speeds from 30 to 100 rps: the availability of the analysis method was thus verified.

Figure 5 shows the results of loss analysis for each rotational speed level.

Figure 5 indicates the values obtained by dividing each loss by the total loss. This figure shows that the rate of leakage loss is largest at 30 rps, which is approx. 2.7 times that at 60 rps. The rate of thrust bearing loss was the next largest. However, comparing the thrust load levels at respective rotational speed values revealed that the thrust load at 30 rps was more than 10% larger than those under conditions at 60 rps or higher. This could presumably be attributed to the fact that the pressure rise in the compression chamber due to leakage was larger than that at 60 rps. It means that thrust bearing loss can be reduced by improving the leakage conditions in the low rotational speed range. In addition, suction heating loss can be expected to decrease by reducing mechanical loss and increasing the amount of refrigerant circulating, thus improving the efficiency beyond the scale of leakage loss improvement.

Leakage loss was small at 100 rps, at which good performance was demonstrated, as shown in the figure.

Quantitative loss analysis of scroll compressors using CO₂ refrigerant was realized by using a simplified model based on a basic test. The authors will improve the performance of systems using this technology and also apply it to other compressors.

References

- (1) Fumiaki Sano et al., A High Reliability Study of the Scroll Compressor, Proceedings of the 1994 Purdue Compressor Conference (1994.7), pp. 199-204.
- (2) NIST, NIST Reference Fluid Thermodynamic Transport Properties – REFPROP Version 7.0 (2002.8).

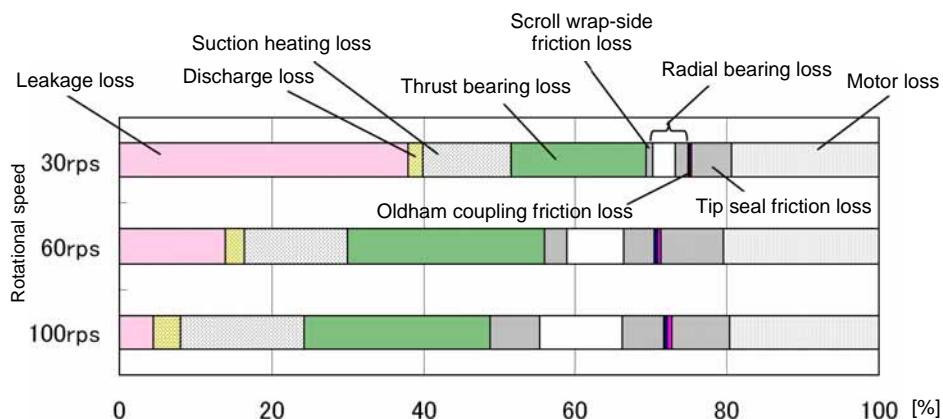


Fig. 5 Analysis of losses in the prototype